10º Congreso de Exploración y Desarrollo de Hidrocarburos
Simposio de Recursos No Convencionales: Hacia una Nueva Convención

DYNAMIC MODELING WORKFLOWS FOR VACA MUERTA WELL SPACING OPTIMIZATION. SIMPLE AND MORE COMPLEX INTEGRATED APPROACHES

Deniz Cakici[1], Tzu-Hao Yeh[1], Yvonne González[1], Ruijian Li[1], Taixu Bai[1]

1: Shell, deniz.cakici@shell.com, tzu-hao.yeh@shell.com, yvonne.gonzalez@shell.com, ruijian.li@shell.com, taixu.bai@shell.com

Keywords: **well spacing, dynamic modeling, interference test, geomechanical modeling**

RESUMEN

¿Simple o Complejo? Dos enfoques de modelaje dinámico integrado para la optimización del espaciamiento de pozos en Vaca Muerta

En este estudio se usaron dos enfoques para sustentar la decisión de espaciamiento de pozos propuesto para el desarrollo de crudo en el área operada por Shell en el *play* Vaca Muerta.

El objeto del estudio es una locación de 3 pozos horizontales completados paralelamente, donde se llevó a cabo una prueba de interferencia para entender los mecanismos y el grado de comunicación entre los mismos. Todos los pozos se navegaron en la misma zona objetivo y contaban con 6 meses de producción al momento de realizar el estudio.

El primer enfoque utilizó un modelaje simple, donde se asume que cada pozo produce de zonas estimuladas simplificadas creadas alrededor de las fracturas hidráulicas (SRV “stimulated rock volume” por sus siglas en inglés). El modelo de simulación de petróleo negro incluyó los 3 pozos, cuyo cotejo histórico fue realizado calibrando la geometría de los SRV y otros parámetros de subsuelo, dentro de un rango de incertidumbre, con el comportamiento de producción de los mismos. El mayor énfasis para el cotejo se asignó al periodo de la prueba de interferencia para lograr el ajuste apropiado de las conexiones y propiedades entre pozos. Luego de completar el cotejo histórico, los parámetros resultantes de reservorio, geometría de fractura y SRV se usaron para el pronóstico de producción y las sensibilidades de espaciamiento. La ventaja principal del modelo simplificado es su velocidad de corrida y la flexibilidad que ofrece para probar diversas combinaciones de geometría de fractura, SRV y propiedades de subsuelo en un corto periodo de tiempo.

El segundo enfoque integró geomecánica con simulación de reservorios para mejorar el entendimiento del comportamiento de producción respecto a las incertidumbres existentes y la distancia de espaciamiento actual entre los pozos. Aunque este enfoque es más complejo y computacionalmente costoso, presenta dos ventajas principales sobre el modelo simplificado de SRV: 1) considera el impacto de espaciamiento sobre el trabajo de completación y la red de fractura creada; 2) utiliza geometrías de fractura hidráulica realistas, las cuales tienen un impacto directo sobre el espaciamiento seleccionado. Para este enfoque, se empleó un simulador avanzado de geomecánica para simular el proceso de fracturamiento hidráulico y para calibrar los modelos con la data de inyección del trabajo de fractura. Una serie de modelos con distintos escenarios de redes de fractura se generaron basados en las incertidumbres de subsuelo identificadas. Estos escenarios junto con las propiedades modeladas, tales como permeabilidad de fractura y distribución de masa de agente de sostén, fueron integradas en un modelo de simulación dinámico. A través de un proceso de cotejo histórico para escenario múltiple se calibraron el resto de los parámetros dinámicos honrando los datos de producción. Después de realizar el cotejo histórico, los parámetros resultantes de reservorio y fractura se usaron en el modelo geomecánico nuevamente para evaluar distintos casos de espaciamiento y diseños de fracturamiento hidráulico. Las nuevas redes de fractura generadas fueron usadas para predecir el impacto de espaciamiento entre pozos y parámetros de completación en la producción de los pozos.

INTRODUCTION

Well spacing is one of the main inputs to the field development plan of Shell operated Argentina Unconventionals asset in the Vaca Muerta Formation of Neuquen Basin. The optimization of well spacing requires a good understanding of well-to-well interactions, which is dominated by the hydraulic fracture geometries and geology (faults, natural fractures, layering, etc.). In order to optimize this key input, asset's first 3-well pad was drilled in 2017. This pad consists of three horizontal wells, which will be called as Western-Well (WW), Center Well (CW) and Eastern Well (EW) in this paper. The lateral trajectories of the wells were drilled in parallel with 320 meters between the wells. Center Well is the first confined well, i.e. a well with an offset producer on both sides, in the asset. All three wells landed at the same target zone.

To capture the potential communication signals between the wells, an interference test was designed. For this purpose, a bottomhole pressure and temperature gauge was installed in each well. These memory gauges started collecting pressure data as soon as the wells started flowing. After three months of production, the interference test was initiated by shutting in the center well. Table 1 summarizes how the wells were operated during the testing period.

	Δt	WW	CW	EW
t = 0	3 months	Producing	Producing	Producing
t = 3 months	2 weeks	Producing	Shut in	Producing
t = 3.5 months	2 weeks	Producing	Producing	Producing
t = 4 months	2 weeks	Shut in	Producing	Producing
t = 4.5 months	2 weeks	Producing	Producing	Producing
t = 5 months	2 weeks	Producing	Producing	Shut in
t = 5.5 months (end of interference test)		Producing	Producing	Producing

Table 1. Statuses of the wells before and during the interference test

Interference test data acquisition was supported by fluid sampling for geochemical fingerprinting. Geochemical analysis is one of the key tools employed by Shell to estimate the effective height of the hydraulic fractures. The geochemical compositions of the produced oil samples from the three wells are compared against the geochemical compositions for oil extracts taken from the cores of nearby vertical wells. The fluid data is matched to the average of the rock data trend at varying depth windows. Based on the matching of depth windows, high-, mid-, and low-confidence fracture heights are estimated. Produced fluids from all three wells were sampled at the start of production, plus before each flowing condition change during the interference test. The analysis for the initial samples when the wells were first turned online are available at the present.

The pressure profiles of the wells until the end of the interference test is shown in Figure 1. As displayed in this plot by the changes in the BHP slopes, WW bottomhole pressure responded strongly when CW was shut in and later brought back online. Similarly, CW reacted strongly when WW was shut in. While the communication between WW and CW was clearly detected, the communication between CW and EW has been subtler. There were changes to the EW BHP slopes when CW was shut in and later put back on production. However, the response was weaker than the one observed at WW. Additionally, when EW was shut in, the change in BHP decline of CW was insignificant. Therefore, it was concluded that CW is strongly connected to the WW, whereas any connection between CW and EW were possible, but not definite.

While the well-to-well connection trends have been detected, there is no supporting data to explain the nature of these connections. To gain more insight on the subsurface mechanisms, two different modeling workflows were employed to match the wells' production performance and interference test results:

1. Simplified SRV model: Uses planar hydraulic fractures created by a commercial simulator's fracture templates. The stimulated reservoir volumes (SRVs) are simply boxes surrounding the hydraulic fractures. The fracture geometries and SRV sizes are history match parameters, which are not directly connected the completion jobs. The model is initiated at the start of the production period.
2. Complex model (with geomechanics based fracture network): Uses complex fracture networks created by a geomechanical simulator, which models the hydraulic fracture completion jobs. The created fracture networks with varying proppant and water placement distributions, as well as and the permeability distribution is, then, used as an input in to the reservoir simulation model.

The main advantage of the simplified model is its speed. Many different combinations of fracture and SRV geometries, as well as subsurface parameters, can be created and tested in a very short amount of time (run times usually measured in minutes for a black-oil model with eight

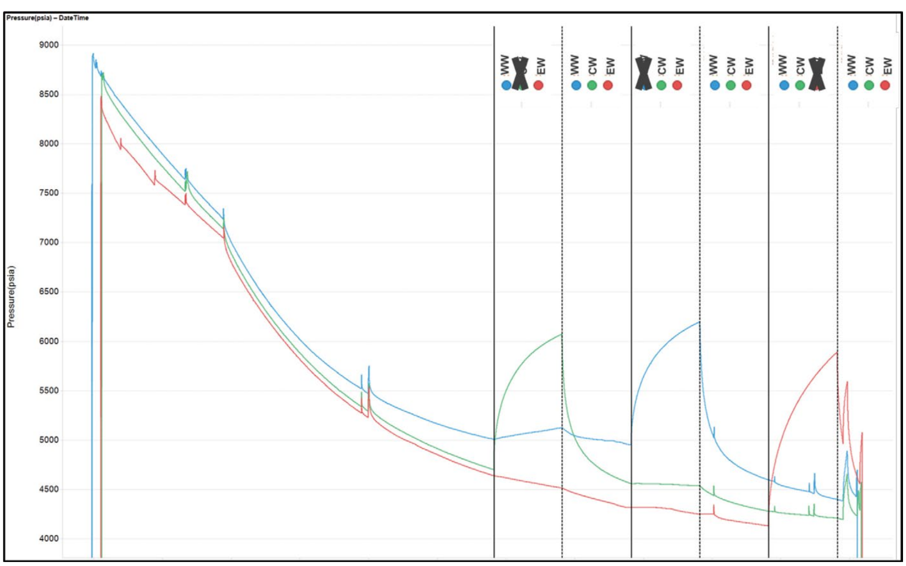

Figure 1. Pressure profiles of the wells until the end of interference test

layers and 3 wells). In contrast, complex modeling workflow is much slower. The geomechanical modeling part takes a significant amount of time (several days to a week) to create the fracture network realizations. Additionally, a fine grid model is required to preserve the complex network created by the geomechanical simulator, and therefore is computationally more expensive compared to simplified SRV reservoir simulation models.

The main advantage of the complex model is its ability to create different fracture networks for varying completion job designs and well spacings. The same completion job may not create the same network, if the wells are placed closer or further apart. By coupling the geomechanical modeling and reservoir simulation, the impact of well spacing on the well performance can be estimated more accurately. In comparison, simplified SRV model is only able to answer what was created at a specific well spacing and a completion design.

Additionally, both modeling approaches have been technologically at different maturity levels. Simple models have been employed and tested in many different projects in the company and the workflows for accurate estimation of EUR ranges are in place. On the other hand, the complex fracture network modeling work has been in progress and only been tested in a few projects.

Considering the pros and cons of each approach and the timeline to provide the inputs to the field development plan, it was decided to carry out both simple and complex modeling workflows in parallel. This enabled the team to compare the history matched results and the forecasted EURs after the completion of both workflows.

In the next two sections, simple and complex modeling workflows and corresponding results are presented.

Simplified SRV Model Based Well Spacing Optimization Methodology

An eight-layer model, covering a total thickness of 90 meters, with varying petrophysical properties in each layer was used in the simulation runs. A single stage, with four perforation clusters, for each well was modeled (Figure 2). The hydraulic fractures were created by using the planar fracture templates available in the reservoir simulation software. As displayed in Figure 2, three distinct regions are created: hydraulic fracture, SRV and matrix. The hydraulic fracture is the planar fracture with very high permeability and low compaction. The matrix is the unstimulated area with the original rock permeability, which is undisturbed by the completion jobs. SRV region is the stimulated rock volume, where the permeability is larger than of the matrix, but lower than the hydraulic fracture permeability. One novel approach employed in this study was using different fracture geometries for each perforation cluster. The fracture half lengths were allowed to vary between 5 and 310 meters. Additionally, each fracture may be surrounded by SRVs at varying sizes or with no SRV at all.

An assisted history match, or AHM, process was carried out to calibrate the models to the actual performance of the wells and the bottomhole pressures acquired. The wells are controlled by oil rate and history match process was run to match the bottomhole pressures. Four best-matched cases are selected for discussion for the remainder of this chapter, which will be referred to as Case #1, #2, #3 and #4.

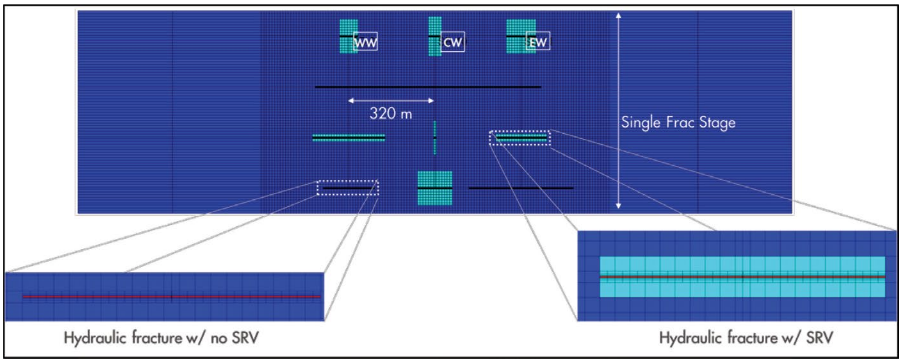

Figure 2. Dynamic model set-up for 3-well single stage model. The dark blue, light blue and red are showing the matrix, SRV and hydraulic fracture blocks, respectively.

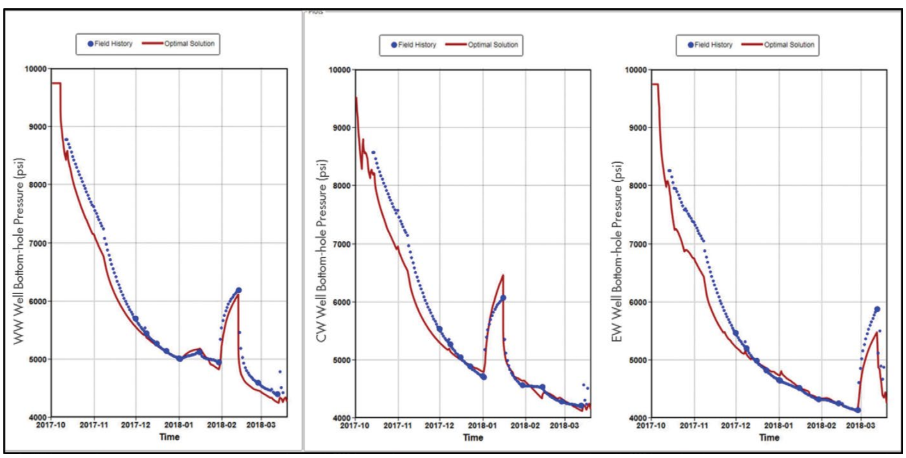

Figure 3. Well bottomhole match all three wells modeled for a single best-match Case #1. Blue dots and red line are for historical and calculated BHPs, respectively.

Figure 3 shows the BHP match quality of Case #1 for all three wells. As seen from this figure, a very good match was achieved not only for the buildup periods, but also for the slope changes at the offset wells during the interference test.

The fracture geometries for the best match cases are shown in Figure 4. Also, the resulting key history match parameters are displayed in Table 2. One key observation is that matching the interference test pressure responses did not require large overlapping SRVs. The pressure responses were created by the long hydraulic fractures connecting the wells, surrounded by narrow SRVs. These long fractures required very large permeabilities, close to 1 darcy for most cases. The hydraulic fracture heights, or Hf's, were in line with the geochemical fingerprinting based high-to-mid confidence estimated values of 25 to 47 meters.

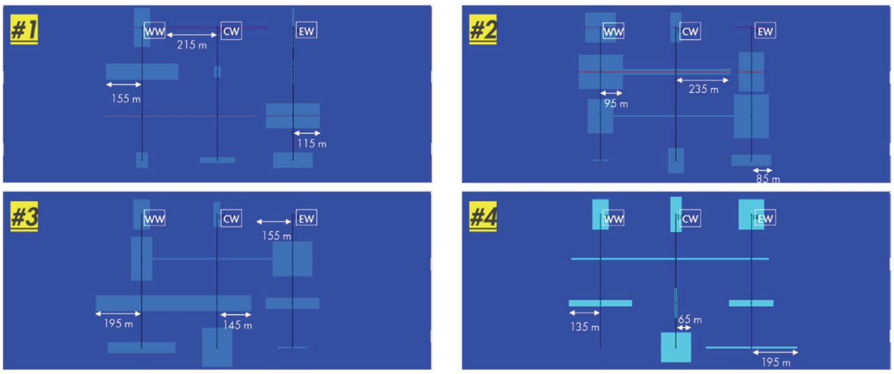

Figure 4. Examples of best matching fracture geometry combinations from the history match process

PARAMETER	#1	#2	#3	#4
WW Hf (m)	47	22	22	47
CW Hf (m)	47	22	22	47
EW Hf (m)	47	22	22	33
Matrix Perm (nd)	31	180	33	54
SRV Perm (nd)	252	480	302	1014
HF Perm (md)	708	407	902	933

Table 2. Major history match parameters for the selected four best-match cases.

After the completion of the history match process, best-matched cases were used in the EUR forecasting and well spacing optimization runs. Figure 5 shows how history matched case #1 was placed in boxes with varying widths to forecast EURs at different well spacing values. The calibrated fracture geometries and other model properties were kept unchanged for all the runs. For case #1, WW and CW were still connected through a single fracture at 410-meter spacing, whereas EW stayed more isolated from the other two wells. As the wells get closer with tighter well spacing, the wells' SRVs started to overlap. At 250-meter spacing wells, as defined in case #1, started acting as a single system.

As mentioned before, the pressure communication between the wells, especially between WW and CW, were observed. Thus, it is not surprising that the pressure communication becomes stronger as the wells get closer. However, it is important to quantify the production impact of the well-to-well connections.

Figure 6 shows two plots to quantify the impact of well spacing on the production. The plot on the left shows the total 3-well EUR change as a function of time for the four selected cases. As seen on this plot, while the EURs vary in a wide range, the reduction in total EUR as a function of well spacing, i.e. the slopes, is similar. The plot on the right shows the production interference discount factors for the four cases as a function of well spacing. For Case #1, moving the well spacing from 410 meters to 310 meters reduces the EUR's by 5%. For the same case, the interference discount is at 11% at 250-meter well spacing. In average, interference discounts for 310- and 250-meter well spacing are 8% and 15%, respectively.

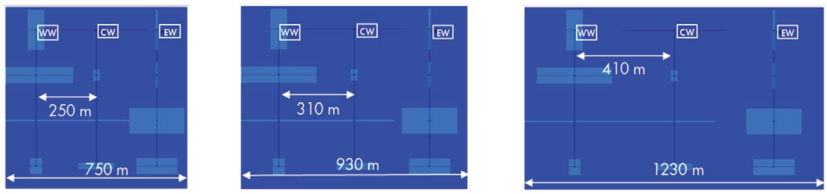

Figure 5. Well spacing scenarios (250, 310 and 410 m, from left to right) based on the fracture geometries of Case #1

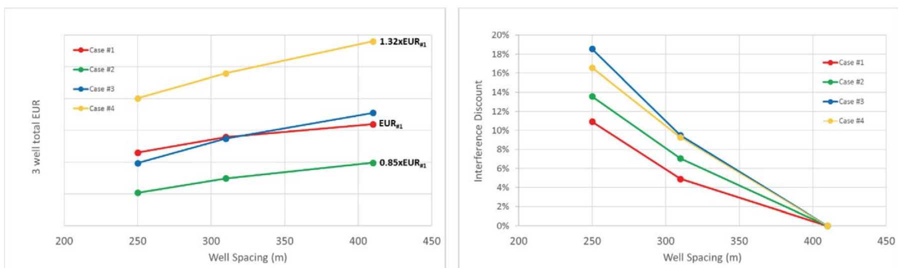

Figure 6. 3-well total EURs (left) and production interference discounts (right) for the best matching cases as a function of well spacing

Well Spacing Optimization Methodology for the Geomechanics Based Complex Fracture Network Model

As mentioned in the introduction section, the simplified SRV modeling-based optimization of well spacing is not capable of capturing the impact of varying well spacings and different completion designs on the size and shape of the fracture networks created. The main assumption carried was that the SRV size that gave the best match will not change when the distance between two wells are changed. In addition, the answers obtained are valid for a single completion job design and may not still be valid if the completion design parameters are modified. In reality, well spacing and completion design are interconnected. The wells can be placed closer and completed by smaller jobs. Or bigger jobs can be pumped at larger spacings. At the end, the economics drives the co-optimization of well spacing and completion design. Thus, a true well spacing optimization requires the inclusion of completion jobs into the optimization workflow.

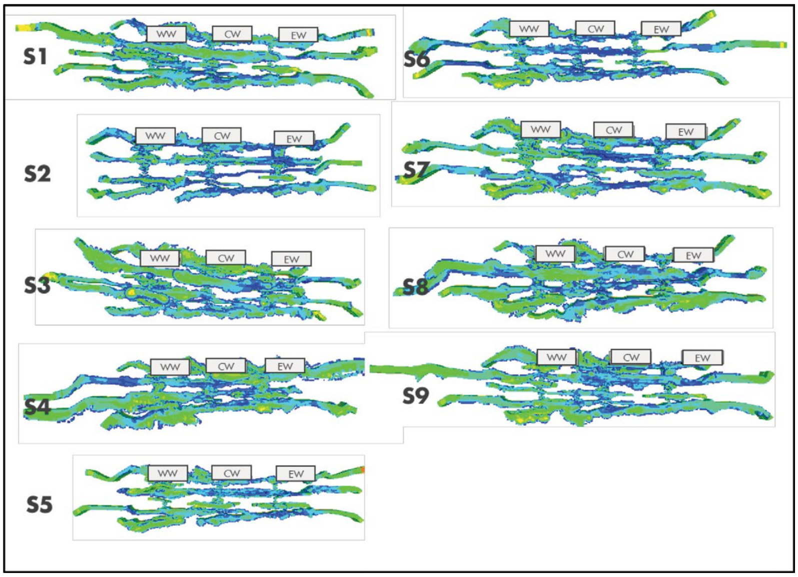

Figure 7. Proppant distribution from the geomechanical simulator for 9 different scenarios

In order to include the completion job designs in the well spacing optimization, a workflow coupling geomechanical and reservoir simulations was employed. This integrated workflow is developed by the Yeh et al. (2018) and starts with the modeling of completion jobs in a geomechanical simulator. Later, the multiple fracture network realizations, calibrated to microseismic and treatment pressures, are imported to the reservoir simulation for history matching. In the history match stage, the fracture network and the reservoir properties are calibrated to match the well performance. Once the reservoir models for the available fracture network scenarios are tuned, they can be used to forecast the well performance for different completion scenarios, each with a different set of fracture network realizations created by geomechanical modeling. In this study, well spacing is added as an extra input parameter to the geomechanical model.

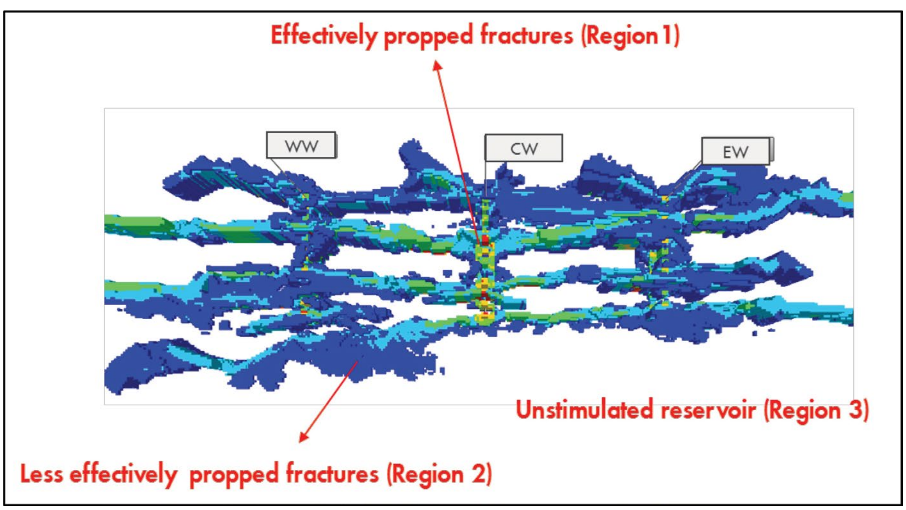

Figure 8. Initialization regions in the dynamic model

Due to the absence of microseismic data on the 3-well pad in discussion, the fracture network realizations in the current study were created by using the input parameters calibrated to a near-by producer. Nine different realizations were created by the geomechanical simulator for the combined 3-well system to cover the uncertainty in the geomechanical model inputs. The model included three hydraulic stages for each well. The proppant distributions of the nine realizations are shown in Figure 7.

For each fracture network scenario, the proppant density and fracture permeability distributions from the geomechanical model were input in a dual-porosity reservoir simulation model. From this point on, the reservoir simulation model treats the fracture network imported as the SRV in the simpler models. However, the SRV size directly coming from the geomechanical model is generally larger than that is observed by the well performance. Thus, by using the proppant density as a threshold, fracture network is divided into two different regions (Figure 8). Region 1, or Effectively Propped Fractures, assigned to the grid blocks with proppant densities over the threshold, has larger fracture permeabilities and increased fracture density and less compaction. In contrast, Region 2, Less Effectively Propped Fractures, with block proppant densities less than the threshold, has lower fracture permeabilities and fracture densities. A third region, being the unstimulated reservoir, surrounds both regions. Due to this setup, three major history match parameters are added with this methodology: proppant threshold (to control the active SRV size), fracture permeability factors (to tune the region permeabilities separately) and the fracture density for each region (to control the flow from matrix blocks to the fracture blocks in the dual porosity system).

The history match process was performed by using Shell's proprietary optimization algorithm. Figure 9 displays BHP match quality of the 3 wells for the best cases. Overall, a very good match was achieved for all the wells, including the three buildups recorded. However, the pressure response of the wells, which were offset to the shut in well, were not captured in this set of history match runs. A specific example to this observation is the pressure increase at WW when CW was closed. This mismatch of the interference test response is an artifact of the way active fractures are defined. In Figure 10, history matched permeability distributions in the landing zone layer for two realizations are shown. As discussed earlier in the simplified modeling workflow learnings, capturing the interference test response in the neighboring wells required long continuous pathways, i.e. high permeability connections, between the wells. In the case of complex models, the high permeability streaks between WW and CW were broken by low permeability blocks. Figure 10 shows two realizations, S4 and S7, with the disconnected well-to-well connections as an example. Since the original fracture networks were a product of the geomechanical modeling, no new connections could be added during the history match process. By simply filtering the original fracture networks, the history match was able to match the build ups, which defined the SRV sizes surrounding the wells. However, the current methodology was unable to capture the well-to-well connections, because the SRV sizes tuned to well performance were smaller and did not create high permeability fractures long enough to connect the wells to each other.

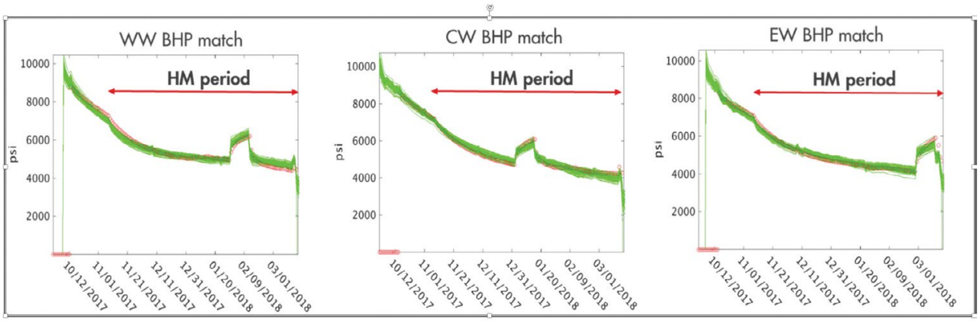

Figure 9. BHP match quality of the best matched cases with geomechanics coupled dynamic model

Figures 11 and 12 give more details on the geometries of the fracture networks created. As mentioned earlier, nine fracture network realizations were used in the history match process. Out of these nine realizations, acceptable history matches were achieved by four of them. Figure 11 displays the proppant density distribution for these four realizations. In each quadrant, the top figure is for the proppant density as created by the geomechanical simulator, and the bottom figure shows the region1, i.e. actively propped fractures, defined by the proppant density threshold after the history match process. The thresholds applied varies between 0.052 and 0.18 lb/ft^2. For all realizations, the region 1 made up a significantly smaller part of the original fracture network created. The resulting fracture heights for the same realizations are displayed in Figure 12. For all

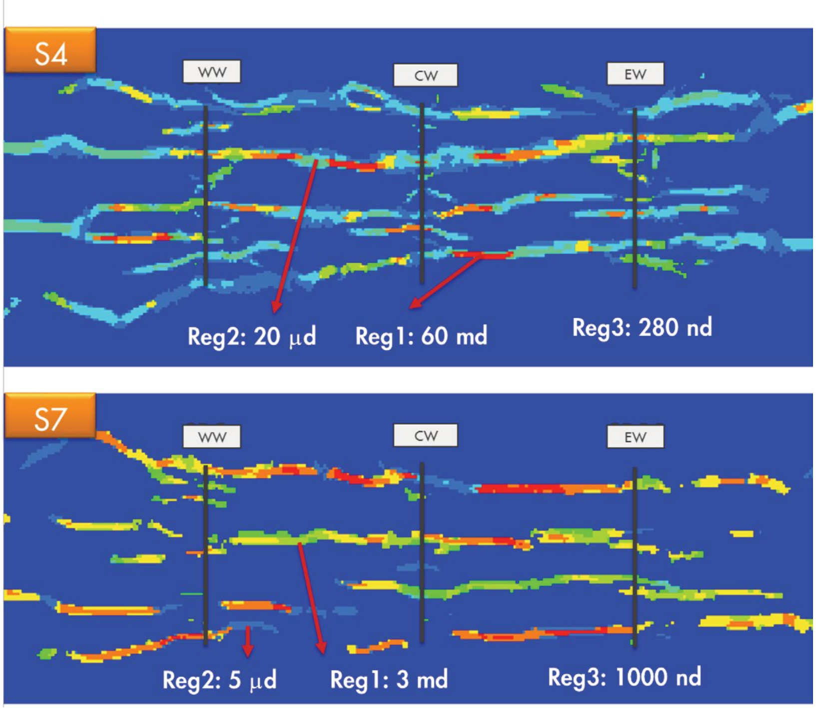

Figure 10. Fracture permeability distribution for Scenarios 4 and 7 (top and bottom, respectively)

the cases, the vertical reach of the region 1 is significantly shorter compared to the original fracture heights from the geomechanical model. In the case of three realizations, the region 1 height estimated is comparable to the fracture heights based on geochemical fingerprinting analysis.

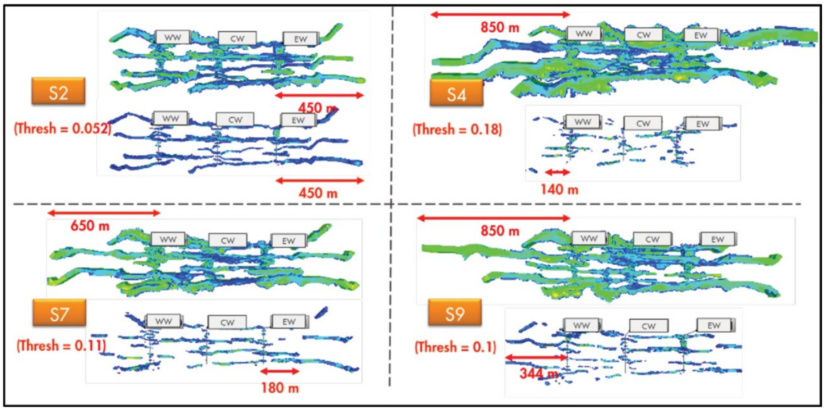

Figure 11. Fracture network scenarios with successful history matching results (top figures in each quadrant) and the proppant mass threshold applied fracture networks that gave the best match (bottom in each quadrant)

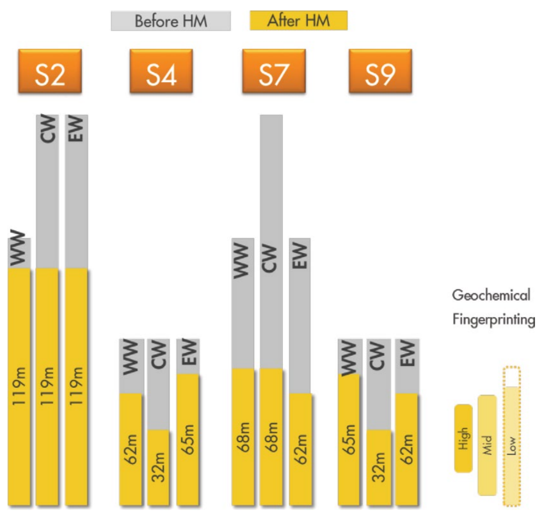

Figure 12. Fracture height comparison of HM results to geochemical fingerprinting based estimates. Gray and orange bars are showing the fracture heights before and after the application of proppant mass threshold, respectively.

Later, the history matched cases were used to forecast the EURs for the wells. Table 3 is comparing the forecasted total 3-well EURs from the geomechanical model based dynamic models to the EURs forecasted by the simplified SRV approach. The complex model based EURs were around 40% larger than the simple model estimations. This significant increase may be due to two factors. First, the SRV created by the geomechanical modeling was much larger than the one used in the simple SRV modeling approach. In fact, the oil in-place volumes of Region

1 of the complex model was comparable to SRVs from the simple models. Second, the width of the complex model is five stages long, with only three stages modeled. This gives an extra drainage volume at the both ends of the simulated stages. Currently, the team is investigating on how to properly discount the impact of these two causes. It was decided to continue the co-optimization of well spacing and completion design study without resolving these issues, since the qualitative performance comparisons of different well spacings and completion designs is agreed to be adequate for fulfilling the field development plan inputs on time.

Simulation Type	Min	Mid	Max
Simple	0.8 x $EUR_{simple,Mid}$	$EUR_{simple,Mid}$	1.3 x $EUR_{simple,Mid}$
Complex	1.1 x $EUR_{simple,Mid}$	1.4 x $EUR_{simple,Mid}$	1.8 x $EUR_{simple,Mid}$

Table 3. Forecasted EUR range comparison of simple and complex models

Finally, well spacing tests were performed by varying completion job designs. Seven completion designs were chosen as listed in Table 4, which cover the well spacing and completion parameters considered for the field development plan. The results presented below used the geomechanical and reservoir simulation input parameters for the realization, S9. The same workflow has not been applied on the other realizations, yet.

Design	Spacing (m)	Stage Length	Proppant Intensity	Water Vol
Base	320	SL_{base}	$PrpInt_{base}$	WV_{base}
CD1	350	2/3 x SL_{base}	1.25 x $PrpInt_{base}$	1.05 x WV_{base}
CD2	400	2/3 x SL_{base}	1.25 x $PrpInt_{base}$	1.18 x WV_{base}
CD3	350	SL_{base}	1.1 x $PrpInt_{base}$	1.09 x WV_{base}
CD4	350	SL_{base}	1.5 x $PrpInt_{base}$	1.45 x WV_{base}
CD5	400	SL_{base}	1.1 x $PrpInt_{base}$	1.09 x WV_{base}
CD6	400	SL_{base}	1.5 x $PrpInt_{base}$	1.45 x WV_{base}
CD7	300	SL_{base}	1.1 x $PrpInt_{base}$	1.09 x WV_{base}

Table 4. Completion designs tested in the geomechanics coupled reservoir models.

Figure 13 compares the fracture networks created by the designs CD3, CD5, and CD7. These three cases use the same completion design parameters at varying well spacings: 300, 350 and 400 meters for CD7, CD3 and CD5, respectively. All cases created an interconnected fracture network, even at a larger well spacings (Figure 13, left). After the application of the threshold, effectively propped fractures, i.e. Region 1, was significantly smaller in the landing zone layer (Figure 13, center). At the same layer, as the wells were placed closer, the Region 1 blocks got more connected. At the deepest layer, where the proppant concentrations are expected to be largest, the wells were connected at all well spacing values, even after the application of the threshold (Figure 13, right).

Table 5 displays the results for all the completion design and well spacing cases. All the designs in consideration for field development plans significantly improved the recovery compared to the base case. The highest recovery was observed for the designs in which proppant intensity and water volume injected were increased the most. Specifically, for well spacing optimization, the

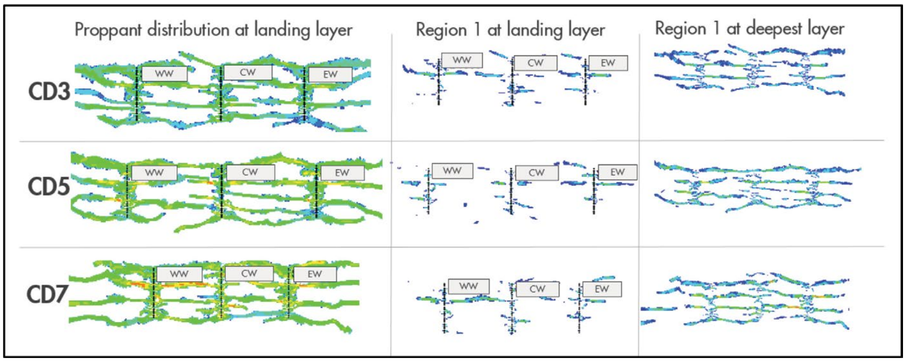

Figure 13. Fracture networks created by same completion parameters, but at varying well spacings

interference discount observed ranged 10 – 14% when the well spacing was reduced to 350 meters from 400 meters. When compared to the interference factors from the simple modeling approach, where the factors are in the 4-6% range for 400 m to 350 m case, complex model based interference factors are significantly higher. However, it should be noted that, the simple modeling approach calculated the well spacing factors for the base completion design, which was not tested for well spacing in the complex workflow due to time limitations. The larger than expected interference factors may be due to larger completion jobs injected in the geomechanical simulations. The future work includes reconciling the differences between the model completions, or confirming which model's estimations are correct.

	Well Spacing	EUR_{min}	EUR_{mid}	EUR_{max}
Base	320 m	0.80 x $EUR_{Base,mid}$	$EUR_{Base,mid}$	1.23 x $EUR_{Base,mid}$
CD1	350 m	1.60 x $EUR_{Base,mid}$	1.91 x $EUR_{Base,mid}$	2.44 x $EUR_{Base,mid}$
CD2	400 m	1.73 x $EUR_{Base,mid}$	2.11 x $EUR_{Base,mid}$	2.74 x $EUR_{Base,mid}$
CD7	300 m	1.40 x $EUR_{Base,mid}$	1.70 x $EUR_{Base,mid}$	2.11 x $EUR_{Base,mid}$
CD3	350 m	1.49 x $EUR_{Base,mid}$	1.75 x $EUR_{Base,mid}$	2.24 x $EUR_{Base,mid}$
CD5	400 m	1.65 x $EUR_{Base,mid}$	2.03 x $EUR_{Base,mid}$	2.59 x $EUR_{Base,mid}$
CD4	350 m	1.76 x $EUR_{Base,mid}$	2.11 x $EUR_{Base,mid}$	2.68 x $EUR_{Base,mid}$
CD6	400 m	2.00 x $EUR_{Base,mid}$	2.35 x $EUR_{Base,mid}$	3.02 x $EUR_{Base,mid}$

Table 5. Comparison of 3-well total EURs for different completion designs

CONCLUSIONS

Two different workflows were completed for a 3-well pad, where strong pressure communication was observed at least between one well pair at 320 meter well spacing.

The first workflow utilizing a simplified SRV approach showed that the well-to-well connections are through very long and thin high permeability streaks. The EURs estimated by the simplified SRV approach were in the expected range of outcomes based on different models applied on other wells in the field. Well-to-well connections, as predicted by the model, do not seem to be a cause of concern at 320-meter well spacing. However, subsurface data acquisition was very limited and the nature of these connections are unknown.

The complex modeling exercise was successful in integrating the geomechanical model outputs into reservoir simulation models and tuning to the well performance histories. The resulting fracture networks, and the forecasted EUR's, were significantly larger than expected. The most likely cause of this overestimation is the way the model is scaled from three fracture stages to the entire well, which will be studied further in the future. The completion jobs with larger proppant intensities and water volumes were tested at different well spacings. The larger completion jobs modeled were successful in increasing the well performances. Additionally, the production interference factors were much larger compared to simplified SRV models. However, there is no one-to-one comparison to simplified SRV models, since complex model based forecasts used enhanced completion job designs.

The current understanding is that the production discount at 320-meter spacing is 4-8% at the current completion job design. This discount factor is likely to be larger when larger completion jobs are pumped. However, since there is no real field data, all available results will be considered in the economic analysis of the development plan and these analyses will be updated with the data coming from future multi-well pads.

ACKNOWLEDGEMENTS

The authors would like to thank Vivek Jain and Ed Kruijs for supporting this study. Also, special thanks to Ricardo Sallas-Porras and Chuck Vecere, for making sure the interference test was executed as planned, to Kristen Boyd, Britt Williams and Patricio Desjardins, for providing the geological inputs required for the models and to Jessica Hinojosa and Sven Scholten, for the geochemical analysis.

REFERENCES

Yeh, T. H., J. Jennings, D. Cakici, J. C. Guerra, M. Durand, B. L. Williams, T. Chen, R. Casillas, V. Jain, H. Liu, R. Li, T. Bai, 2018, "An Integrated Geomechanics-Reservoir Simulation Workflow for Completion Design Optimization", URTeC, Houston, TX, USA, 23-25 July 2018